Available online at www.sciencedirect.com

jmr&t Journal of Materials Research and Technology

journal homepage: www.elsevier.com/locate/jmrt

Original Article

Investigation of severe lunar environmental conditions on the physical and mechanical properties of lunar regolith geopolymers

Shima Pilehvar [a], *Marlies Arnhof* [b], *Andreas Erichsen* [a], *Luca Valentini* [c], *Anna–Lena Kjøniksen* [a,*]

[a] *Faculty of Engineering, Østfold University College, P.O. Box 700, Halden, 1757, Norway*

[b] *Advanced Concepts Team, ESA European Space Research and Technology Centre, Keplerlaan 1, TEC-SF, Noordwijk, 2201AZ, the Netherlands*

[c] *Department of Geosciences, University of Padua, Padua, 35131, Italy*

ARTICLE INFO

Article history:
Received 30 September 2020
Accepted 29 January 2021
Available online 5 February 2021

Keywords:
Geopolymer
Lunar regolith simulant
Urea
Vacuum
3D printing

ABSTRACT

3D-printing of geopolymers produced from lunar regolith is an interesting option for space *in situ* habitats. In this study, the influence of the severe lunar environmental conditions such as extreme temperature variations and vacuum on the physical and mechanical properties of lunar regolith geopolymers were investigated. Additionally, the effect of different amounts of urea as a geopolymer superplasticizer was evaluated. Utilization of urea was found to reduce the water needed to reach the same workability by up to 32%. Extrudability tests showed that mixtures containing 3 wt.% urea could be continuously extruded, and built up into a five layer structure without any noticeable deformation. Addition of urea decreased the compressive strength after exposure to the temperature variations of one lunar day–and–night cycle during curing. However, urea can prevent concrete degradation after the lunar cycle by increasing the amounts of air voids. X-ray tomography showed that the porosity became higher when urea was added to the samples, and increased markedly when the samples were cured in vacuum.

1. Introduction

The possibility of moon colonisation has emerged since the Apollo missions in the 1960s. Utilizing the moon as an intermediate station to explore outer space has been considered by major space agencies such as the National Aeronautics and Space Administration (NASA) and the European Space Agency (ESA).

Several options for building a human settlement on the moon have been suggested, such as utilizing lunar regolith to fabricate cement/concrete for *in-situ* construction, transporting construction materials or completed habitation modules from earth, and constructing an underground

* Corresponding author.
E-mail address: anna.l.kjoniksen@hiof.no (A. Kjøniksen).

https://doi.org/10.1016/j.jmrt.2021.01.124

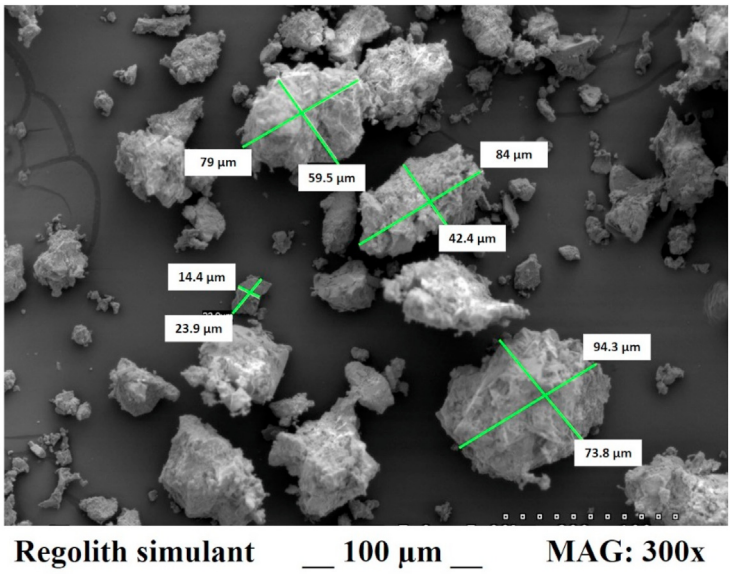

Fig. 1 – SEM images of the lunar regolith simulant.

habitat by digging into the lunar surface [1]. However, due to the extremely high expense of transporting materials to the moon, it is necessary to minimize the weight of components that have to be imported from earth [2]. Therefore, both NASA and ESA follow the policy of *in-situ* resource utilization by applying local lunar materials for construction [3].

Geopolymers (inorganic alumino-silicate polymers) are utilized on earth as a more environmentally friendly substitute for ordinary Portland cement [4]. Geopolymers can be produced from lunar regolith, due to the similarity in chemical composition with terrestrial geopolymer binders [5]. This material is interesting for lunar construction due to its excellent resistance against extreme temperature fluctuation, and adequate radiation shielding [6,7].

3D printing equipment could be shipped to extra-terrestrial locations for printing lunar regolith geopolymers into the desired structures [8,9]. In order to be suitable for 3D printing, the fresh properties of the construction composites need to exhibit appropriate extrudability, buildability and workability [10]. Generally, fresh geopolymer composites have poor workability due to the high viscosity of the alkaline solution [11]. Increasing the water content or adding a superplasticizer improves the workability, but causes a reduction in compressive strength of the hardened geopolymers [12]. The moisture content in the lunar regolith is estimated to be between 0.3% and 1% [13]. Although there is some water available on the moon [14–19], it is a very limited resource. It is therefore necessary to minimize the amount of water used the lunar geopolymer building materials. Utilizing an easily accessible chemical admixture that can increase the workability and reduce the water demand of lunar regolith geopolymers for 3D printing is therefore essential. In a recent article [5], we showed that urea can act as a superplasticizer for geopolymers, probably due to its ability to break hydrogen bonds [20]. Since urea is a major component of urine, it is readily available anywhere there are humans.

Severe environmental conditions like a large temperature variation between day and night, vacuum, and solar radiation are considered as the main obstacles for construction on the moon [21]. A day–and–night cycle on the moon lasts for over 29 earth days, with long periods of extreme hot and cold temperatures from 114 °C to −170 °C [22]. High vacuum and the absence of oxygen also influence the mechanical properties of lunar constructions. In addition to enhanced water evaporation, high vacuum can affect the surface cleanliness of lunar particles and may result in a change of shear strength [23].

The aim of this paper is to investigate the severe lunar environmental conditions such as the extreme temperature variations and vacuum on the physical and mechanical properties of lunar regolith geopolymers for 3D printing. Additionally, the effect of different amounts of urea as a geopolymer superplasticizer is evaluated. The designed lunar geopolymer mixtures are simultaneously examined at ambient conditions to compare the data for both lunar and terrestrial construction purposes, and to evaluate which effects are due to the vacuum conditions.

2. Experimental setup

2.1. *Materials*

DNA-1 lunar regolith simulant was provided by Dini Engineering srl for Monolite UK ltd in the premises of Cascine di Buti (Pisa), Italy. It was developed for ESA as a substitute to the lunar mare regolith. The main chemical compounds of this lunar regolith simulant are 47.79 wt. % SiO_2, 19.16 wt. % Al_2O_3, 8.75 wt. % Fe_2O_3, and 8.28 wt. % CaO [5]. XRD data show that the crystallinity is about 75 vol.%, which is in agreement with the lunar regolith glass content of 1–25 vol.% [24]. Scanning electron microscopy (SEM) images of the lunar regolith

Table 1 – Mixture design of the lunar regolith samples. LG denotes lunar geopolymer, the numbers indicate the percentage urea (with respect to the regolith mass), and W indicates samples with the same workabilities.

Sample denotation	Lunar regolith simulant (g)	Water (g)	NaOH pellets (g)	Urea (g)	alk:reg[a]	W:S[b]
LG0W	1000	288	162	0	0.45	0.25
LG3W	1000	224	126	30	0.35	0.19
LG5W	1000	205	115	50	0.32	0.17
LG0	1000	224	126	0	0.35	0.20
LG3	1000	224	126	30	0.35	0.19
LG5	1000	224	126	50	0.35	0.19

[a] alk:reg = alkaline solution to regolith ratio.
[b] W:S = water to solid ratio.

simulant are shown in Fig. 1, where the regolith particles are much sharper than their terrestrial counterparts due to the bombardment by meteorites in the lunar environment [25].

Sodium hydroxide pellets purchased from VWR, Norway, were used for preparation of the alkaline solution. Urea (in powder form, 99.5% purity) supplied by VWR, Norway, was utilized as an accessible lunar chemical admixture to evaluate the workability and water demand of lunar geopolymer (LG) mixtures.

2.2. *Mixing, casting and curing procedures*

For all LG mixtures containing different percentages of urea, 12 M (480 g/L) sodium hydroxide was utilized as the alkaline solution. In order to check how much water could be saved by adding urea, samples with the same workabilities were first compared. These are denoted LG0W, LG3W, and LG5W for samples containing 0, 3, and 5% urea, respectively. For the remaining experiments, an optimal alkaline solution to regolith ratio of 0.35 was selected. Different urea dosages corresponding to 0, 3, and 5% of the lunar regolith mass were added and denoted LG0, LG3, and LG5, respectively. The mixture design of all samples is shown in Table 1. The sample containing 3% urea has the same composition for both types of experiments (LG3W = LG3).

For specimen preparation, regolith and alkaline solution with 0, 3, and 5 wt. % of urea were mixed together for 8 min to reach a homogenous and uniform mixture. After mixing, the fresh paste was cast into molds of 4 × 4 × 4 cm size. A vibration machine was used for 1 min to remove air trapped inside the specimens. After casting, half of the LG samples were pre-cured in a vacuum thermal chamber (Binder VD23 Vacuum Oven) at 0.01 mbar, while the others were pre-cured in an ambient thermal chamber. A pre-curing temperature of 80 °C for 3 h was applied for both vacuum and ambient chambers. After demolding, the samples were exposed to the lunar surface temperature variation throughout a lunar cycle in accordance with Malla and Brown [22], who showed that the temperature profile varies between 387 K (114 °C) and 102 K (−171 °C) on the moon (Fig. 2). Due to the lack of suitable equipment, the lower temperature in the current work was limited to −80 °C. The utilized temperature profile is shown in Fig. 2. The samples were kept in an exicator for maintaining a vacuum environment during the lunar cycle.

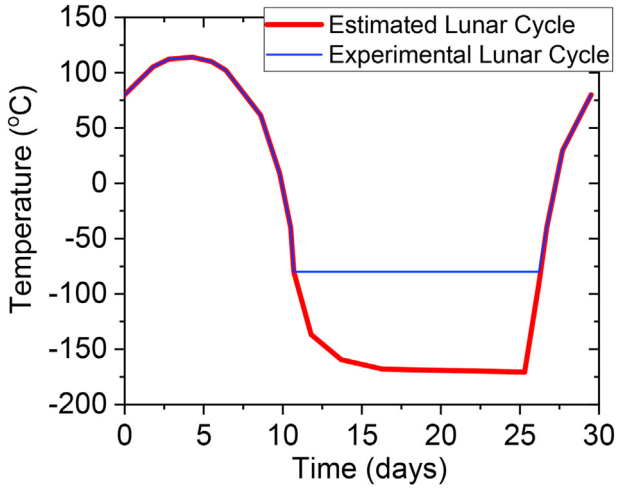

Fig. 2 – Estimated lunar temperature variation [22], and the experimental lunar cycle utilized in this work (limited due to lack of sub −80 °C freezer).

2.3. *Methods*

2.3.1. *Water reduction*

Due to the limited access of water on the moon, it is essential to keep the water content in the LG mixture as low as possible while retaining sufficient workability and strength. Mini slump experiments were utilized to quantify the reduced amount of water needed to retain the same workability in the presence of urea. A flow table (63-L0040/Gx Flow table, Controlsgroup) with a cone (diameter of 10.16 cm at the base and 6.09 cm at the top) was utilized, and each sample was dropped 25 times before measuring the sample diameter as illustrated in Fig. 3. The reduced water demand in the presence of urea was determined by comparing the amount of water needed to reach a fixed diameter deviation of 0.5 cm between the diameter of the sample and the base diameter of the cone.

2.3.2. *Extrudability*

Extrudability is one of the critical parameters for 3D printing, and shows whether the materials can be extruded as a continuous and homogenous filament through the nozzles without any disruption. The extrudability of LG mixtures was performed by means of a high-pressure syringe pump (Fusion 6000, Chemyx, Inc.) with a constant pump rate of 25 ml/min at

room temperature (RT) and in a vacuum thermal chamber at 80 °C. In addition, to quantify the early age properties of the mixtures such as workability, consistency, and flow behavior, rheological characterization is required [26]. Yield stress and viscosity of the material can be considered as flow properties inside any pipe or complex shaped channel [27]. Therefore, rotational rheological measurements of fresh LG0, LG3, and LG5 were carried out using an Anton Paar MCR302 rheometer (Austria) at 80 °C. The mixtures were tested using a PP25/P2 (parallel plate) plate–plate measuring system (diameter: 25 mm; inset I-PP50/SS) After loading the pre-heated mixture into the 80 °C rheometer plate, the sample was kept in the rheometer at 80 °C for 60 s, to ensure that the samples have the same temperature history. The samples were measured from 10^{-4} to 100 s^{-1} using a logarithmic ramp with 1 s per data point and 61 data points. Yield stress values were estimated utilizing the Bingham model: $\tau = \tau_0 + \mu_p \dot{\gamma}$, where τ is the shear stress, τ_0 is the yield stress, μ_p is the plastic viscosity, and $\dot{\gamma}$ is the shear rate [28]. The data were fitted in the low shear rate range ($\dot{\gamma} < 0.01\ s^{-1}$) where the curves are linear.

2.3.3. *Buildability*

The buildability of fresh LG mixtures was examined by means of a high-pressure syringe pump (Fusion 6000, Chemyx, Inc.) with a constant pump rate of 25 ml/min.

2.3.4. *Setting time*

To characterize the initial and final setting times of LG after adding different percentages of urea, a Vicat needle test was performed by a manual Vicat needle apparatus in accordance with EN 196–3. After placing the fresh mixture in the mold, the experiment was carried out in both vacuum and ambient thermal chambers at a temperature of 80 °C with an interval of 15 min. The initial setting time is the time when the needle penetration is less than 39 mm whereas the final setting time is the moment when the needle penetrates the sample to a depth of 0.5 mm.

2.3.5. *Compressive strength and mass loss*

The compressive strength tests for LG specimens before and after simulated lunar temperature variations in both vacuum and ambient pressure were performed at 20 °C in accordance with EN 12190, using a digital compressive strength test machine (QUASAR 100, GALDABINI). Additionally, the percentage of LG mass loss was calculated to examine the influence of temperature variation on the LG degradation.

2.3.6. *Microstructural study*

X-ray microtomography (XCT) scans were performed on cylindrical samples (1 cm diameter) before and after simulated lunar temperature variations. XCT measurements were performed with lab scanner equipped with a W source (operated at 85 kV) and a CCD detector of 4000 × 2700 pixels. The samples were positioned at 75.18 mm from the source and 133.57 mm from the detector, with a camera binning of 2 × 2 pixels, resulting in a final voxel linear size of 6.5 μm. An angular step of 0.3° over 180° total rotation and an exposure time of 975 ms per projection were used. Tomographic reconstruction was performed using the FDK algorithm [29]. The reconstructed images consist of 1200 vertically stacked cross-sections. Image processing was performed by the ImageJ software on representative volumes of 214 mm^3 [30], and consisted of a first step of conversion of grayscale to binary images by means of the "triangle method" [31] with the aim of segmenting isolated pores. The size of each pore was then calculated and pore size distributions obtained.

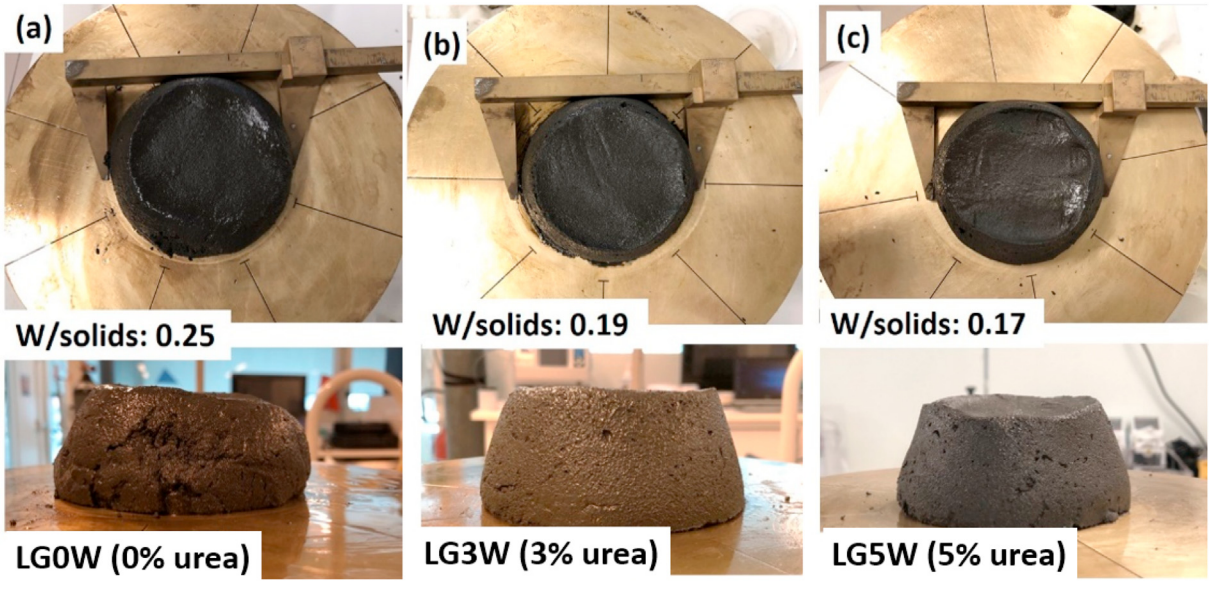

Fig. 3 – Mini slump measurements of the flowability of the geopolymers. To retain the same workability in all mixtures, the water to solids ratio has been varied. a) Without urea, water to solid ratio = 0.25, b) 3% urea with respect to regolith, water to solid ratio = 0.19, c) 5% urea with respect to regolith, water to solid ratio = 0.17.

3. Results and discussions

3.1. Water reduction

The water to geopolymer solids ratio needed to reach the same diameter deviation (0.5 cm) of the mini slump experiments for mixtures containing 0 (LG0W), 3 (LG3W), and 5 (LG5W) wt. % urea, is shown in Fig. 4a. Increasing the amount of urea from 0 to 5 wt. %, reduced the water demand by 32% (Fig. 4b). As can be seen from Fig. 3, LG0 has visible cracks and low consistency, although the flowability was the same as the other samples. Urea can break hydrogen bonds [32]. The addition of urea to the geopolymers can therefore reduce the amount of water needed to achieve a good workability of the samples [5], which is critical for construction on the moon.

3.2. Extrudability

The extrudability tests of LG0, LG3, and LG5 (0, 3, and 5 wt. % urea) at a constant alkaline solution to regolith ratio of 0.35 were carried out at RT under 1 atm and in a vacuum thermal chamber at 80 °C (Fig. 5). The extrudability of the mixtures was noticeably affected by the urea concentration. The mixture without urea (LG0) exhibited a too high stiffness and cohesion for extrusion, which led to clogging of the nozzle. Therefore, LG0 is not presented in Fig. 5. As can be seen in Fig. 5a and b, LG3 (3 wt. % urea) and LG5 (5 wt. % urea) could be continuously extruded from the pump nozzle in the lab environment. In the vacuum environment, LG3 could be easily extruded through the narrow extruding tube (1 cm in diameter) as an almost continuous filament (see Fig. 5c). However, LG5 did not keep a good enough consistency, and was disrupted into smaller sections during extrusion in vacuum (Fig. 5d). For both LG3 and LG5, there are many visible voids on the filament after extruding in vacuum. According to Li et al. [33], vacuum dehydration treatment causes the water to evaporate faster and induces agglomeration, causing more voids to appear on the surface. In addition, urea can release NH_3 and H_2 gases at 80 °C [34]. At higher urea contents (5 wt. %), larger amounts of released NH_3 and H_2 gases can be sucked out by the vacuum. This might cause excess void creation and disruption of the extruded filaments. However, it should be noted that the syringe pump in this experiment was stationary, and printing of the circle shaped mixtures was conducted by means of a rotary disk inside the vacuum chamber, while the geopolymer mixture was extruded from outside the vacuum chamber through a tube. Therefore, the extrudability test in vacuum is poorly controlled, which might affect the results.

The rheological behavior of the fresh paste is very important to successfully extrude the paste. Since the sample without urea was too hard with poor workability, we were not able to measure the rheology of this sample. As can be seen from Fig. 6, the viscosity of the pastes is reduced with about 1 order of magnitude when the urea concentration is raised from 3 to 5 wt.%, while the shear thinning behavior of the two samples is similar. In addition, the yield stress decreases from 42 ± 3 Pa (3 wt.% urea) to 2.6 ± 0.5 Pa (5 wt.% urea). This illustrates that the addition of urea significantly decreases the viscosity of the samples as well as the yield stress. For good extrudability, it is important that these factors are low. However, for 3D printing it is essential that the zero-shear viscosity (viscosity as the shear rate approaches zero) is not too low, since this will cause the samples to deform during the printing process.

3.3. Buildability

In addition to the extrudability, the buildability of LG3 and LG5 (extrudable mixtures) was also examined to ensure the stability of the structures in the time between extrusion and solidification. As mentioned in section 2.2, the sample without urea was too stiff and viscous to be extruded and built layer by layer. Due to the lack of control on the syringe pump in the vacuum chamber, this experiment was performed only at ambient conditions. Fig. 7 illustrates that increasing the percentage of urea from 3 to 5 wt.% results in poorer buildability, as is evident by the visual deformation and collapse of the LG5 sample. A higher amount of urea results in higher fluidity and less viscous mixtures, as shown in Fig. 6. Accordingly, the LG5 mixture started deforming after the deposition of the third layer (Fig. 7b), while LG3 (containing 3 wt.% urea) was still stable after depositing a fifth layer (Fig. 7a).

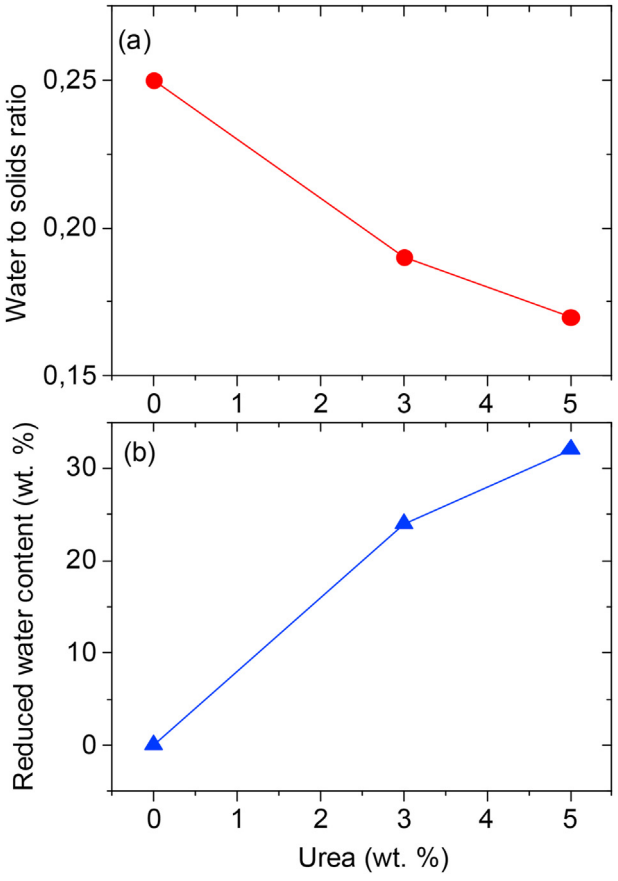

Fig. 4 – (a) The water to geopolymer solids ratio needed to obtain a constant mini slump at different urea concentrations, (b) reduced water content compared to the sample without urea.

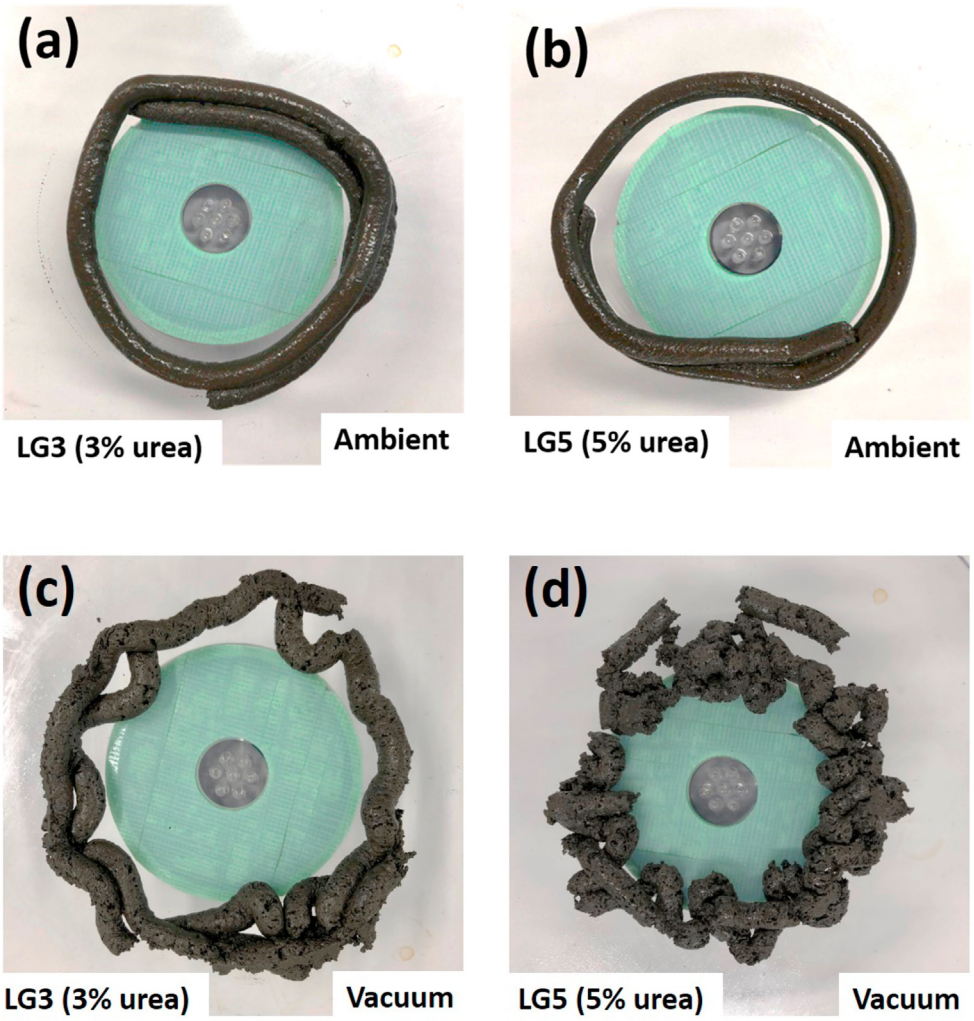

Fig. 5 – Extrudability of mixtures containing (a) 3 wt.% urea (LG3) and (b) 5 wt.% urea (LG5) at ambient conditions, (c) 3 wt.% urea (LG3) and (d) 5 wt.% urea (LG5) at vacuum conditions.

3.4. *Setting time*

Fig. 8 shows the effect of different percentages of urea on the initial and final setting times of lunar geopolymers at 80 °C. The experiment was carried out in both vacuum and ambient pressure to investigate how the environments affects the hardening process of lunar geopolymers. The initial setting time is longer (except for 5% urea) in vacuum than at ambient pressure. A vacuum treatment at elevated temperatures can accelerate the evaporation of free water available in the geopolymer, and consequently increase the viscosity of the mixture. While a reduced amount of water shortens both the initial and final setting times [35], the increased viscosity can slow down the geopolymerization rate, and accordingly prolong the initial setting time [35]. However, when the urea solutions are heated up to 80 °C, NH_3 and H_2 gasses can be emitted [34], which can contribute to the shorter initial setting time in vacuum after addition of high amounts (5%) of urea (LG5). The final setting time is dominated by the reduced amount of water available [35], and is therefore shorter at vacuum conditions.

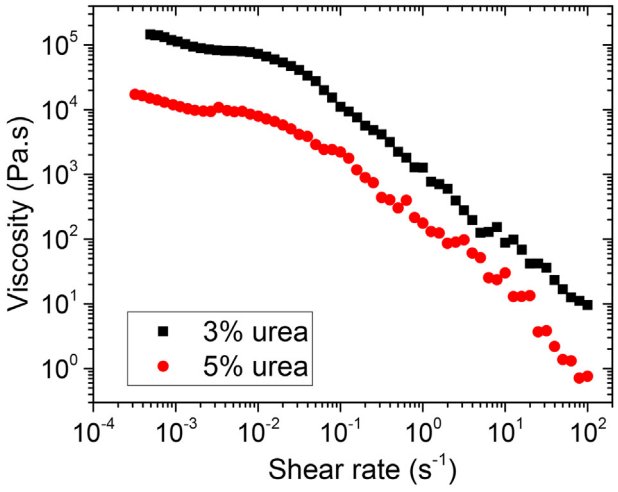

Fig. 6 – Shear rate dependency of the viscosity of pastes containing 3 and 5 wt.% urea.

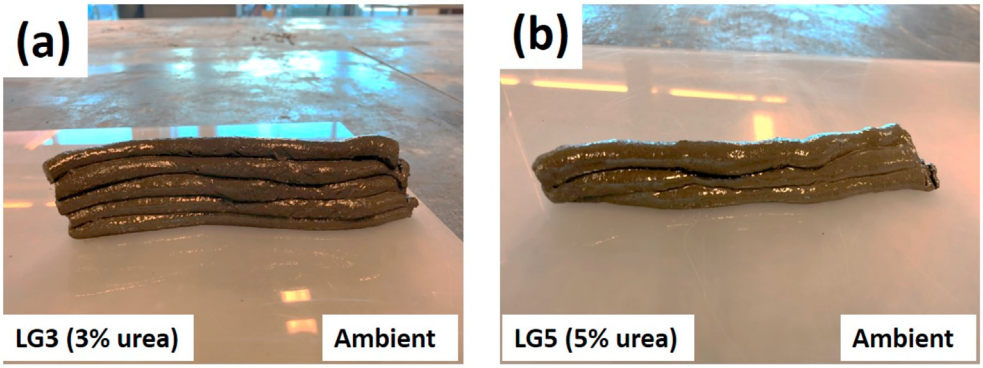

Fig. 7 – Buildability of (a) mixture containing 3% urea (LG3) and (b) mixture containing 5% urea (LG5) at ambient conditions. Extruded through a 1 cm tube.

According to a previous study [5], urea exhibits promising properties as a superplasticizer and retarder for 3D-printing of lunar geopolymers by breaking hydrogen bonds and delay the setting time. In agreement with this, incorporating urea into the lunar geopolymer postpones both the initial and final setting times compared to the samples without any urea addition both at vacuum and ambient pressure. This allows the mixture to be sufficiently workable and extrudable during 3D printing. However, adding higher amounts of urea (LG5) causes the mixture to be too fluid and the filaments to collapse after printing (Fig. 7b).

3.5. *Microstructural study*

2D X-ray micro-tomography cross-sectional slices obtained from samples LG0 and LG5 cured in both ambient pressure and vacuum are shown in Fig. 9. Features with vanishing X-ray attenuation, such as voids and cracks, are displayed in dark colour. In order to quantify any difference between the samples, the void size distributions are displayed in Fig. 10,

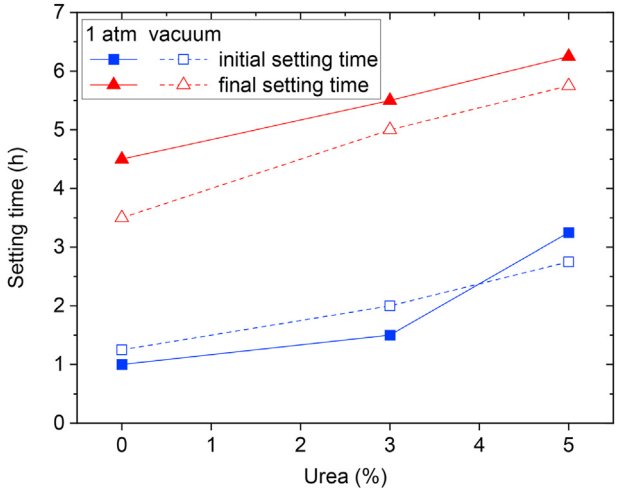

Fig. 8 – Initial setting and final setting time at 80 °C of lunar geopolymers containing 0, 3, and 5 wt.% urea in vacuum and at ambient pressure.

and overall volumes of voids as well as volume increments induced by urea additions are shown in Fig. 11. Except for the sample cured in vacuum before the lunar cycles, porosity increases markedly with the addition of urea (Fig. 11). Moreover, curing in vacuum induces a striking rise in porosity (Fig. 9; Fig. 11a). This is probably caused by water evaporation inside the samples, resulting in voids that do not escape to the surface due to the high viscosity of the samples. Since urea can release NH_3 and H_2 gases at 80 °C [34], the porosities are even more enhanced in the presence of urea. The size distributions of the samples cured in vacuum has a higher fraction of small voids than the samples cured at 1 atm (Fig. 10). This is probably caused by tiny gas bubbles formed within the samples due to lower boiling points at reduced pressures. As is evident from Fig. 9, a few large voids with irregular shape are also formed at vacuum conditions, suggesting that several smaller voids are joined together into larger cavities. There are no clear trends in the size distributions (Fig. 10) when the urea concentration is increased. Since void sizes are affected by viscosities (Fig. 6) as well as gasses released from urea and from water evaporation, the overall picture is too complex to result in a clear trend. At ambient pressure and low urea concentrations, the porosities are increased after the lunar cycle (Fig. 11a). However, the samples that already exhibit a high porosity before the lunar cycle have a better resistance against the extreme thermal variations of the lunar cycle. Voids within concrete samples are known to improve the frost resistance of concrete, since they can act as expansion reservoirs when water freezes [36,37]. This can explain why the lunar cycle does not induce the same porosity increase for the high porosity samples. The geopolymer reaction proceeds throughout at least parts of the lunar cycle, which might explain why some of the samples have a reduced porosity after the cycle.

3.6. *Compressive strength*

Fig. 12 presents the compressive strength of LG0, LG3, and LG5 before and after a lunar temperature variation throughout a lunar cycle (Fig. 2) in vacuum and at ambient pressure. The compressive strength increased for all samples after the lunar

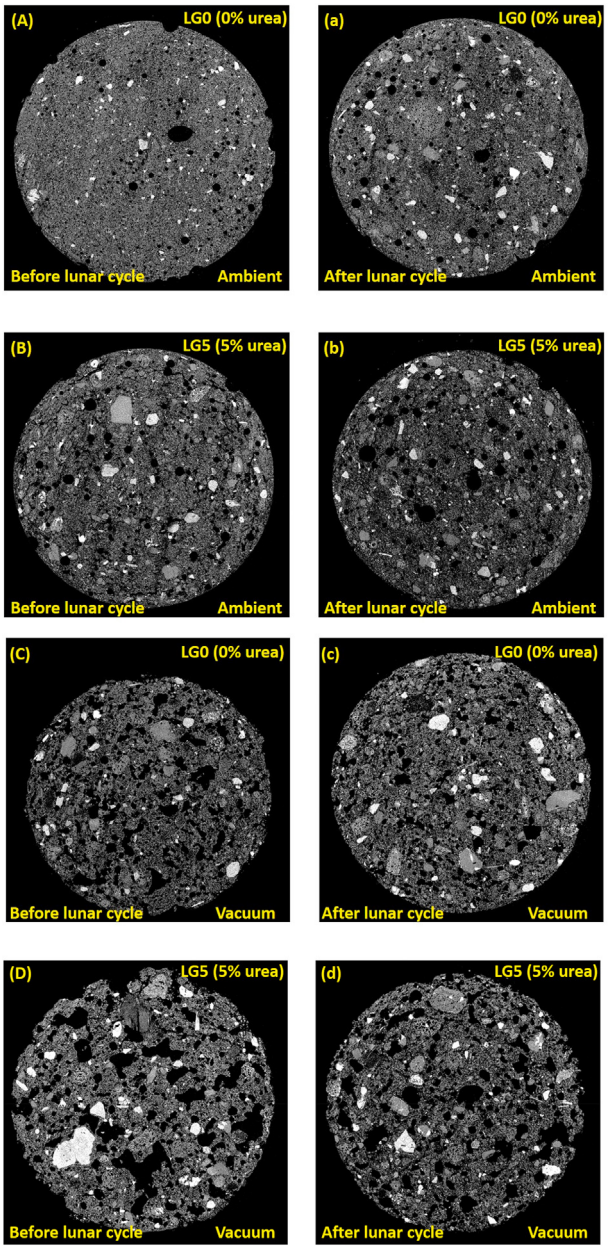

Fig. 9 – X-ray tomography images of (A) LG0 before lunar cycle, (a) LG0 after lunar cycle, (B) LG5 before lunar cycle, (b) LG5 after lunar cycle cured under atmospheric pressure and (C) LG0 before lunar cycle, (c) LG0 after lunar cycle, (D) LG5 before lunar cycle, and (d) LG5 after lunar cycle, cured under vacuum. The field of view is approximately 1 cm.

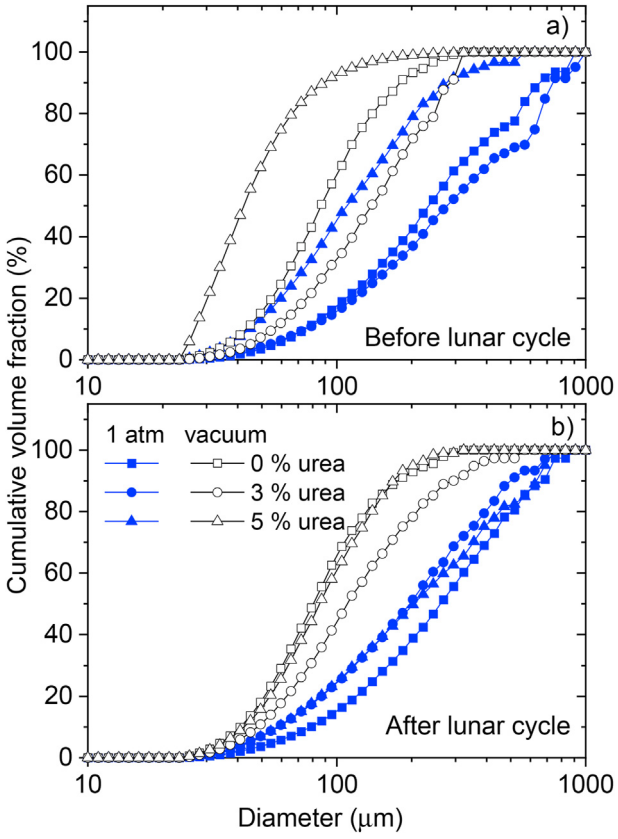

Fig. 10 – Analysis of voids from X-ray tomography. Cumulative volume fractions of the voids (a) before and (b) after the lunar cycle.

cycle, compared to the initial values after only 3 h precuring at 80 °C. Although the reaction rate is expected to be very slow or non-existent at the lowest temperatures, the poly-condensation reaction of the geopolymer continues throughout parts of the lunar cycle. This causes an overall increase in compressive strength, despite the negative effect of the extreme freeze–thaw cycle on the geopolymer structure. The increase in compressive strength after the lunar day–and–night cycle is much higher at ambient conditions, illustrating that the vacuum contributes to deterioration of the geopolymer strength. The lower compressive strength for the samples cured in a vacuum are in agreement with the enhanced porosities of the vacuum samples (Fig. 11a).

When increasing the percentage of urea, the porosity becomes higher (Fig. 9; Fig. 11), and accordingly the compressive strength is reduced (Fig. 12a). This strength reduction was highest after the lunar cycle in vacuum (Fig. 12b), although the porosity increase is largest for the sample that is cured at ambient pressure before the lunar cycle (Fig. 11b). Since the compressive strength decreases both with increasing porosity and with a higher fraction of large pores [38], this might be related to differences in pore size distributions (Fig. 10). Fig. 13 illustrates the relation between the compressive strength and the porosity of the samples. The general trend is, as expected, with a linear decline in strength as the porosity becomes higher [38]. The deviations of some of the points are probably caused by variations in pore size distributions (Fig. 10).

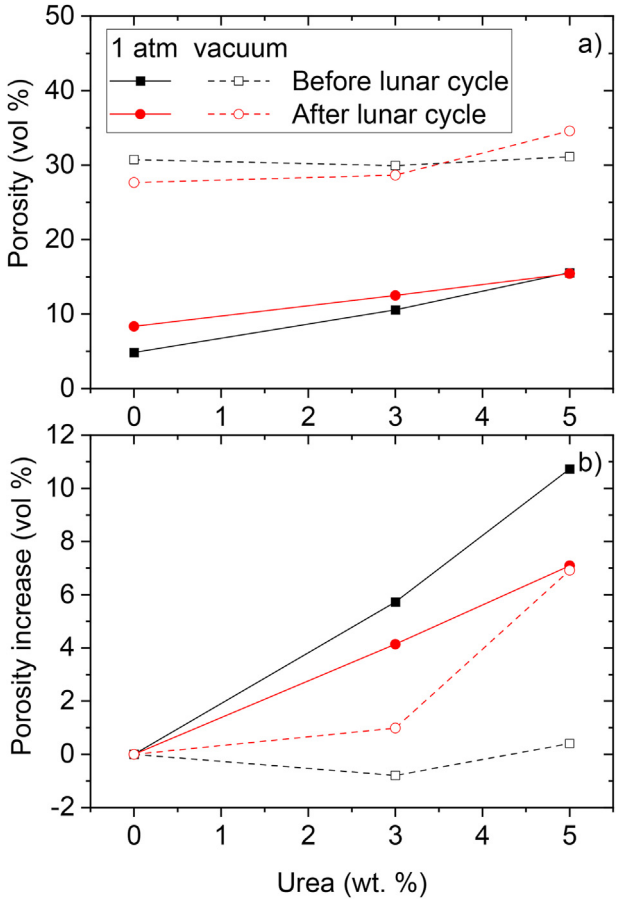

Fig. 11 – Analysis of voids from X-ray tomography. (a) porosity of the lunar geopolymers, (b) porosity increase after urea addition.

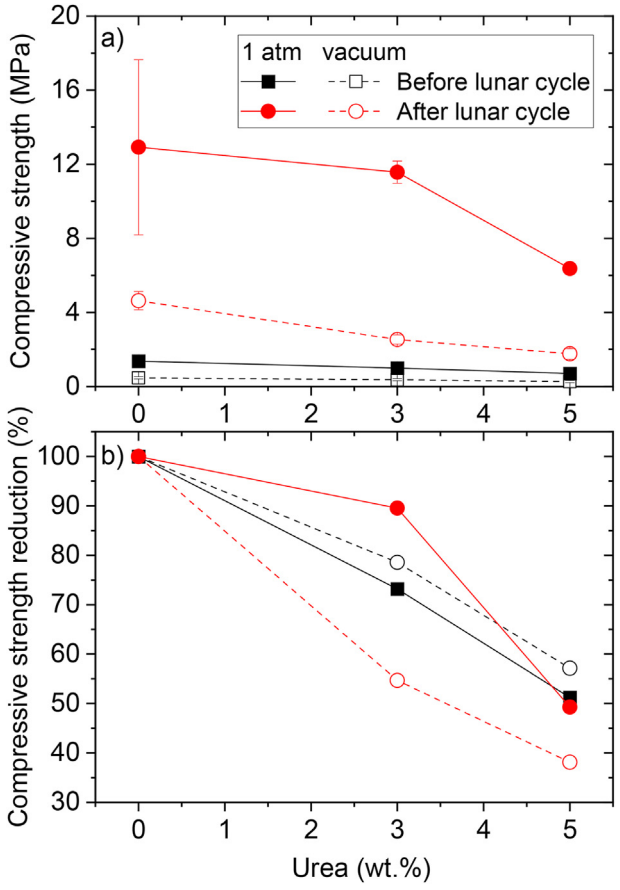

Fig. 12 – (a) Compressive strength of lunar geopolymer before and after a lunar cycle at vacuum and at ambient pressure. (b) The percentage reduction of the compressive strength after adding urea. The samples were pre-cured for 3 h at 80 °C before starting the lunar cycle.

3.7. *Mass loss*

The mass loss for all LG specimens was examined to evaluate the effect of urea addition on the geopolymer erosion after exposure to a lunar day–and–night cycle. Fig. 14 shows that for LG samples cured at vacuum conditions, the specimens were only slightly influenced by the harsh environment of the lunar temperature cycle, which led to a negligible mass loss. Adding urea has little effect on the mass loss for the samples cured in a vacuum. For LG cured at ambient pressure the results are very different from the vacuum conditions. The mass loss for the LG sample without any urea was around 10% after one lunar cycle at ambient pressure. However, after adding 5 wt.% urea the specimens exhibited a mass increase (negative mass loss) after the temperature cycle. This mass increase might be attributed to the absorption of moisture from the freeze–thaw cycle at ambient pressure [36]. According to Łaźniewska-Piekarczyk [39], adding superplasticizers can enhance air void formation, and thereby provide durability for the sample during freezing–thawing cycles. Utilizing urea results in a substantial increase of the porosity in comparison with the sample without any admixture (Fig. 11a), and can therefore prevent concrete degradation during the lunar temperature cycle.

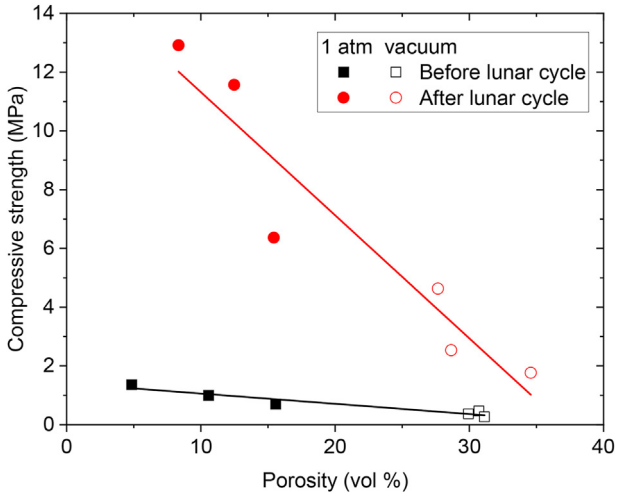

Fig. 13 – Compressive strength as a function of porosity. The lines are linear fits to the data before and after the lunar cycle.

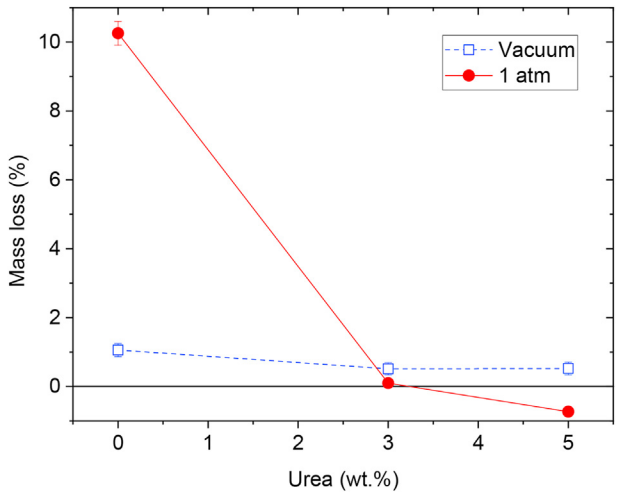

Fig. 14 – Mass loss after one lunar cycle.

4. Conclusions

In this study, the extreme temperature variations and vacuum of the lunar environment, as well as different amounts of urea as a superplasticizer were examined with respect to the effect on the physical and mechanical properties of lunar regolith geopolymers for 3D printing. The following conclusions can be drawn from this work:

1. Adding urea can reduce the water needed to reach the same workability by up to 32%.
2. The extrudability of the mixtures was noticeably influenced by the urea addition. LG3 (3 wt. % urea) could be continuously extruded from the pump nozzle both at 1 atm and at vacuum conditions, whereas LG5 (5 wt % urea) did not keep a good enough consistency during extrusion in the vacuum. The sample without urea was too viscous for extrusion.
3. The addition of urea significantly decreases the viscosity and the yield stress of the samples. For 3D printing the zero-shear viscosity should not be too low, since this could deform samples during the printing process.
4. A buildability test at lab conditions illustrated that an increase in urea concentration from 3 to 5 wt.% results in poorer buildability, as was evident by the visual deformation and collapse of the LG5 sample.
5. Incorporating urea into the geopolymer mixture postponed both the initial and final setting times in comparison with the samples without any urea at both vacuum and ambient pressures. However, the initial setting time was longer (except for 5% urea) in vacuum than at ambient pressure. The final setting time is shorter at vacuum conditions.
6. The porosity of the samples increased when urea was added to the samples. The porosity is much higher for the samples cured at vacuum conditions.
7. The compressive strength increased for all samples after the lunar day–and–night cycle, compared to the samples precured for 3 h at 80 °C. The increase in compressive strength after the lunar cycle is much higher at ambient conditions, which demonstrates that the vacuum causes the geopolymer deterioration. Adding urea decreased the compressive strength at both vacuum and ambient pressure.
8. LG samples cured at vacuum conditions were only slightly influenced by the harsh environment of the lunar cycle, which led to a negligible mass loss. Adding urea has little effect on the mass loss for the samples cured in a vacuum.

Declaration of Competing Interest

The authors declare that they have no known competing financial interests or personal relationships that could have appeared to influence the work reported in this paper.

Acknowledgement

This work is the result of an Ariadna study, a joint collaborative research project between the Faculty of Engineering at Østfold University College and the Advanced Concepts Team (ACT) of the European Space Agency (ESA). We would like to thank Rino Nilsen for technical assistance.

REFERENCES

[1] Cesaretti G, Dini E, De Kestelier X, Colla V, Pambaguian L. Building components for an outpost on the Lunar soil by means of a novel 3D printing technology. Acta Astronaut 2014;93:430. https://doi.org/10.1016/j.actaastro.2013.07.034.
[2] NASA. Advanced Space transportation program: paving the highway to space.
[3] Davis G, Montes C, Eklund S. Preparation of lunar regolith based geopolymer cement under heat and vacuum. Adv Space Res 2017;59:1872. https://doi.org/10.1016/j.asr.2017.01.024.
[4] Davidovits J Geopolymer chemistry and applications. Saint-Quentin, France: Institute Géopolymère; 2011.
[5] Pilehvar S, Arnhof M, Pamies R, Valentini L, Kjøniksen A-L. Utilization of urea as an accessible superplasticizer on the moon for lunar geopolymer mixtures. J Clean Prod 2020;247:119177. https://doi.org/10.1016/j.jclepro.2019.119177.
[6] Montes C, Broussard K, Gongre M, Simicevic N, Mejia J, Tham J, et al. Evaluation of lunar regolith geopolymer binder as a radioactive shielding material for space exploration applications. Adv Space Res 2015;56:1212. https://doi.org/10.1016/j.asr.2015.05.044.
[7] Sun P, Wu H-C. Chemical and freeze–thaw resistance of fly ash-based inorganic mortars. Fuel 2013;111:740. https://doi.org/10.1016/j.fuel.2013.04.070.
[8] Leach N. 3D printing in space. Architect Des 2014;84:108. https://doi.org/10.1002/ad.1840.
[9] Goulas A, Binner JG, Harris RA, Friel RJ. Assessing extraterrestrial regolith material simulants for in-situ resource utilisation based 3D printing. Applied Materials Today 2017;6:54. https://doi.org/10.1016/j.apmt.2016.11.004.
[10] Le TT, Austin SA, Lim S, Buswell RA, Gibb AG, Thorpe T. Mix design and fresh properties for high-performance printing

concrete. Mater Struct 2012;45:1221. https://doi.org/10.1617/s11527-012-9828-z.
[11] Pilehvar S, Cao VD, Szczotok AM, Valentini L, Salvioni D, Magistri M, et al. Mechanical properties and microscale changes of geopolymer concrete and Portland cement concrete containing micro-encapsulated phase change materials. Cement Concr Res 2017;100:341. https://doi.org/10.1016/j.cemconres.2017.07.012.
[12] Chindaprasirt P, Chareerat T, Sirivivatnanon V. Workability and strength of coarse high calcium fly ash geopolymer. Cement Concr Compos 2007;29:224. https://doi.org/10.1016/j.cemconcomp.2006.11.002.
[13] Benaroya H, Bernold L. Engineering of lunar bases. Acta Astronaut 2008;62:277. https://doi.org/10.1016/j.actaastro.2007.05.001.
[14] Hendrix AR, Hurley DM, Farrell WM, Greenhagen BT, Hayne PO, Retherford KD, et al. Diurnally migrating lunar water: evidence from ultraviolet data. Geophys Res Lett 2019;46:2417. https://doi.org/10.1029/2018gl081821.
[15] Chen Y, Zhang Y, Liu Y, Guan Y, Eiler J, Stolper EM. Water, fluorine, and sulfur concentrations in the lunar mantle. Earth Planet Sci Lett 2015;427:37. https://doi.org/10.1016/j.epsl.2015.06.046.
[16] Hauri EH, Saal AE, Rutherford MJ, Van Orman JA. Water in the Moon's interior: truth and consequences. Earth Planet Sci Lett 2015;409:252. https://doi.org/10.1016/j.epsl.2014.10.053.
[17] McCubbin FM, Vander Kaaden KE, Tartèse R, Klima RL, Liu Y, Mortimer J, et al. Magmatic volatiles (H, C, N, F, S, Cl) in the lunar mantle, crust, and regolith: abundances, distributions, processes, and reservoirs. Am Mineral 2015;100:1668. https://doi.org/10.2138/am-2015-4934CCBYNCND.
[18] Barnes JJ, Kring DA, Tartèse R, Franchi IA, Anand M, Russell SS. An asteroidal origin for water in the Moon. Nat Commun 2016;7:11684. https://doi.org/10.1038/ncomms11684.
[19] Dubinskii AY, Popel SI. Water formation in the lunar regolith. Cosmic Res 2019;57:79. https://doi.org/10.1134/s0010952519020047.
[20] Usha R, Ramasami T. Effect of hydrogen-bond-breaking reagent (urea) on the dimensional stability of rat tail tendon (RTT) collagen fiber. J Appl Polym Sci 2002;84:975. https://doi.org/10.1002/app.10262.
[21] Benvenuti S, Ceccanti F, De Kestelier X. Living on the moon: topological optimization of a 3D-printed lunar shelter. Nexus Netw J 2013;15:285. https://doi.org/10.1007/s00004-013-0155-7.
[22] Malla RB, Brown KM. Determination of temperature variation on lunar surface and subsurface for habitat analysis and design. Acta Astronaut 2015;107:196. https://doi.org/10.1016/j.actaastro.2014.10.038.
[23] Perko HA, Nelson JD, Sadeh WZ. Surface cleanliness effect on lunar soil shear strength. J Geotech Geoenviron Eng 2001;127:371. https://doi.org/10.1061/(ASCE)1090-0241(2001)127:4(371).
[24] Schleppi J, Gibbons J, Groetsch A, Buckman J, Cowley A, Bennett N. Manufacture of glass and mirrors from lunar regolith simulant. J Mater Sci 2019;54:3726. https://doi.org/10.1007/s10853-018-3101-y.
[25] Colwell J, Batiste S, Horányi M, Robertson S, Sture S. Lunar surface: dust dynamics and regolith mechanics. Rev Geophys 2007;45:RG2006. https://doi.org/10.1029/2005RG000184.
[26] Pacheco-Torgal F, Castro-Gomes J, Jalali S. Alkali-activated binders: a review. Part 2. About materials and binders manufacture. Construct Build Mater 2008;22:1315. https://doi.org/10.1016/j.conbuildmat.2007.03.019.
[27] Choi MS, Kim YJ, Kim JK. Prediction of concrete pumping using various rheological models. International Journal of Concrete Structures and Materials 2014;8:269. https://doi.org/10.1007/s40069-014-0084-1.
[28] Yahia A, Khayat KH. Analytical models for estimating yield stress of high-performance pseudoplastic grout. Cement Concr Res 2001;31:731. https://doi.org/10.1016/S0008-8846(01)00476-8.
[29] Feldkamp L, Davis L, Kress J. Practical cone-beam algorithm. JOSA A 1984;1:612.
[30] Schneider CA, Rasband WS, Eliceiri KW. NIH Image to ImageJ: 25 years of image analysis. Nat Methods 2012;9:671.
[31] Zack GW, Rogers WE, Latt SA. Automatic measurement of sister chromatid exchange frequency. J Histochem Cytochem 1977;25:741. https://doi.org/10.1177/25.7.70454.
[32] Wei H, Fan Y, Gao YQ. Effects of urea, tetramethyl urea, and trimethylamine N-oxide on aqueous solution structure and solvation of protein backbones: a molecular dynamics simulation study. J Phys Chem B 2010;114:557. https://doi.org/10.1021/jp9084926.
[33] Li W, Lemougna PN, Wang K, He Y, Tong Z, Cui X. Effect of vacuum dehydration on gel structure and properties of metakaolin-based geopolymers. Ceram Int 2017;43:14340. https://doi.org/10.1016/j.ceramint.2017.07.190.
[34] Jones JM, Rollinson AN. Thermogravimetric evolved gas analysis of urea and urea solutions with nickel alumina catalyst. Thermochim Acta 2013;565:39. https://doi.org/10.1016/j.tca.2013.04.034.
[35] Pilehvar S, Cao VD, Szczotok AM, Carmona M, Valentini L, Lanzón M, et al. Physical and mechanical properties of fly ash and slag geopolymer concrete containing different types of micro-encapsulated phase change materials. Construct Build Mater 2018;173:28. https://doi.org/10.1016/j.conbuildmat.2018.04.016.
[36] Pilehvar S, Szczotok AM, Rodríguez JF, Valentini L, Lanzón M, Pamies R, et al. Effect of freeze-thaw cycles on the mechanical behavior of geopolymer concrete and Portland cement concrete containing micro-encapsulated phase change materials. Construct Build Mater 2019;200:94. https://doi.org/10.1016/j.conbuildmat.2018.12.057.
[37] Coussy O, Monteiro PJM. Poroelastic model for concrete exposed to freezing temperatures. Cement Concr Res 2008;38:40. https://doi.org/10.1016/j.cemconres.2007.06.006.
[38] O'Farrell M, Wild S, Sabir BB. Pore size distribution and compressive strength of waste clay brick mortar. Cement Concr Compos 2001;23:81. https://doi.org/10.1016/S0958-9465(00)00070-6.
[39] Łaźniewska-Piekarczyk B. The influence of selected new generation admixtures on the workability, air-voids parameters and frost-resistance of self compacting concrete. Construct Build Mater 2012;31:310. https://doi.org/10.1016/j.conbuildmat.2011.12.107.